An energy function based design of second order sliding modes for Automatic Generation Control ⋆

Sebastian Trip * **Michele Cucuzzella** ** **Antonella Ferrara** **
Claudio De Persis *

* *ENTEG, Faculty of Mathematics and Natural Sciences, University of Groningen, Nijenborgh 4, 9747 AG Groningen, the Netherlands. (e-mail: s.trip@rug.nl; c.de.persis@rug.nl).*
** *Dipartimento di Ingegneria Industriale e dell'Informazione, University of Pavia, via Ferrata 1, 27100 Pavia, Italy. (e-mail: michele.cucuzzella@gmail.com; a.ferrara@unipv.it)*

Abstract: This paper proposes a decentralized Second Order Sliding Mode (SOSM) control strategy for Automatic Generation Control (AGC) in power networks, where frequency regulation is achieved, and power flows are controlled towards their desired values. This work considers a power network partitioned into control areas, where each area is modelled by an equivalent generator including second order turbine-governor dynamics, and where the areas are nonlinearly coupled through the power flows. Asymptotic convergence to the desired state is established by constraining the state of the power network on a suitable sliding manifold. This is designed relying on stability considerations made on the basis of an incremental energy (storage) function. Simulation results confirm the effectiveness of the proposed control approach.

Keywords: Sliding mode control, Decentralized control, Stability of nonlinear systems, Power systems stability.

1. INTRODUCTION

As a result of power mismatch between generation and load demand, the frequency in a power system can deviate from its nominal value. Whereas primary droop control is utilized to prevent destabilization of the network, the frequency is controlled back to its nominal value by the so-called 'Automatic Generation Control' (AGC). In an AGC scheme, each Control Area (CA) determines its Area Control Error (ACE) and changes the setpoints to the governor accordingly to compensate for local load changes and to maintain the scheduled tie line power flows. Due to the increasing share of renewable energy sources, it is however unsure if the existing implementations are still adequate (Apostolopoulou et al. (2016)).

To cope with the increasing uncertainties affecting a CA and to improve the controllers performance, advanced control techniques have been proposed to redesign the conventional AGC schemes, such as Model Predictive Control (Ersdal et al. (2016)), adaptive control (Zribi et al. (2005)) and fuzzy control (Chang and Fu (1997)). In this work we propose a new control strategy based on the Sliding Mode (SM) control methodology, which has been previously used in the literature to improve the conventional AGC schemes (Mi et al. (2013), Dong (2016)), possibly together with fuzzy logic (Ha (1998)), genetic algorithms (Vrdoljak et al. (2010)), disturbances observers (Mi et al. (2016)), linear matrix inequalities (LMI) based control techniques (Prasad et al. (2015)) and passivity based approach (Cucuzzella et al. (2017)).

SM control is a well known robust control approach, especially useful to control systems subject to modelling uncertainties and external disturbances (Utkin (1992), Edwards and Spurgen (1998)). This also holds for Second Order SM (SOSM) control (Bartolini et al. (1999)), where not only the sliding variable but also its first time derivative are steered to zero in a finite time, thus providing, under suitable working conditions, an intrinsic chattering alleviation effect (Utkin and Lee (2006)).

In this paper, we adopt the model of a power network partitioned into control areas, having an arbitrarily complex and meshed topology. The generation side is modelled by an equivalent generator including second order turbine-governor dynamics, where the proposed *decentralized* control scheme continuously adjusts the governor set point. To be able to control the power system using continuous control signals, which can be beneficial in field implementations, the well known Suboptimal SOSM (SSOSM) control algorithm (Bartolini et al. (1998a)) is exploited. Moreover, the convergence to the sliding manifold is obtained neither measuring the power demand, nor using load observers.

When the nonlinear power system is constrained to the designed sliding manifold, the convergence towards the desired state is established relying on a suitable incremental energy function (Trip et al. (2016)) and Lyapunov argu-

⋆ This is the final version of the accepted paper submitted for inclusion in the Proceedings of the International Federation of Automatic Control (IFAC) World Congress, Toulouse, France, July, 2017.

ments. Indeed, an incremental energy function based stability analysis suggests the design of the sliding manifold. Finally, the case study considered in the paper shows the effectiveness of the proposed controller and demonstrates that the combined use of SM control and other nonlinear control techniques can provide new insights and control strategies.

2. NETWORK MODEL

Consider a power network consisting of n interconnected control areas. The network topology is represented by a connected and undirected graph $\mathcal{G} = (\mathcal{V}, \mathcal{E})$, where the nodes $\mathcal{V} = \{1, ..., n\}$, represent the control areas and the edges $\mathcal{E} \subset \mathcal{V} \times \mathcal{V} = \{1, ..., m\}$, represent the transmission lines connecting the areas. The topology can be described by its corresponding incidence matrix $\mathcal{B} \in \mathbb{R}^{n\times m}$. Then, by arbitrary labeling the ends of edge k with a '+' and a '−', one has that

$$\mathcal{B}_{ik} = \begin{cases} +1 & \text{if } i \text{ is the positive end of } k \\ -1 & \text{if } i \text{ is the negative end of } k \\ 0 & \text{otherwise.} \end{cases}$$

Representing a control area with an equivalent generator and load, the governing dynamic equations of the i-th node are the following [1]:

$$\begin{aligned} \dot{\delta}_i &= f_i \\ \dot{f}_i &= -\frac{1}{T_{pi}} f_i + \frac{K_{pi}}{T_{pi}} P_{ti} - \frac{K_{pi}}{T_{pi}} P_{di} \\ &\quad - \frac{K_{pi}}{T_{pi}} \sum_{j\in\mathcal{A}_i} \frac{\overline{V}_i \overline{V}_j}{X_{ij}} \sin(\delta_i - \delta_j), \end{aligned} \tag{1}$$

where $\mathcal{A}_i$ is the set of nodes connected to the i-th node by transmission lines. Note that we assume that the network is lossless, which is generally valid in high voltage transmission networks where the line resistance is negligible. Moreover, P_{ti} in (1) is the power generated by the i-th plant, and it can be expressed as the output of the following second order dynamic system that describes the behaviour of both the governor and the turbine:

$$\begin{aligned} \dot{P}_{ti} &= -\frac{1}{T_{ti}} P_{ti} + \frac{1}{T_{ti}} P_{gi} \\ \dot{P}_{gi} &= -\frac{1}{R_i T_{gi}} f_i - \frac{1}{T_{gi}} P_{gi} + \frac{1}{T_{gi}} u_i. \end{aligned} \tag{2}$$

The main symbols used in systems (1) and (2) are described in Table 1.

To study the power network we write system (1) and the turbine-governor dynamics in (2) for all nodes $i \in \mathcal{V}$ as

$$\begin{aligned} \dot{\eta} &= \mathcal{B}^T f \\ T_p K_p^{-1} \dot{f} &= -K_p^{-1} f + P_t - P_d - \mathcal{B}\Gamma\sin(\eta) \\ T_t \dot{P}_t &= -P_t + P_g \\ T_g \dot{P}_g &= -R^{-1} f - P_g + u, \end{aligned} \tag{3}$$

where $\eta = \mathcal{B}^T\delta \in \mathbb{R}^m$, $f \in \mathbb{R}^n$, $P_t \in \mathbb{R}^n$, $P_g \in \mathbb{R}^n$, $\Gamma = \text{diag}\{\Gamma_1, \ldots, \Gamma_m\}$, with $\Gamma_k = \overline{V}_i \overline{V}_j / X_{ij}$, $\sin(\eta) = (\sin(\eta_1), \ldots, \sin(\eta_m))^T$, $P_d \in \mathbb{R}^n$ and $u \in \mathbb{R}^n$. Matrices T_p, T_t, T_g, K_p, R are suitable $n \times n$ diagonal matrices.

[1] For the sake of simplicity, the dependence of the variables on time t is omitted througout this paper.

Table 1. Description of the used symbols

Symbol	Description
δ_i	Voltage angle
f_i	Frequency deviation
P_{ti}	Turbine output power
P_{gi}	Governor output
T_{pi}	Time constant of the control area
T_{ti}	Time constant of the turbine
T_{gi}	Time constant of the governor
K_{pi}	Gain of the control area
R_i	Speed regulation coefficient
$\overline{V}_i$	Constant voltage
X_{ij}	Line reactance
u_i	Control input
P_{di}	Unknown power demand

To permit the controller design in the next sections, the following assumption is made on the disturbances (*unknown* loads) and the available measurements:

Assumption 1. (**Available measurements.**) The variables f_i, P_{ti}, P_{gi} and the power flow $(\mathcal{B}\Gamma\sin(\eta))_i$ are locally available at control area i. The unmatched disturbance P_{di} is unknown, constant and can be bounded as

$$|P_{di}| \le \mathcal{D}_i, \tag{4}$$

where $\mathcal{D}_i$ is a positive constant available at control area i.

3. PROBLEM FORMULATION

In this section we formulate two objectives of automatic generation control. The first objective is concerned with the steady state frequency deviation.

Objective 1. (**Frequency regulation**)

$$\lim_{t\to\infty} f(t) = \mathbf{0}. \tag{5}$$

The second objective is to maintain the scheduled net power flows in a control area, where the net power flow is the total power flow exchanged by a control area.

Objective 2. (**Maintaining scheduled net power flows**)

$$\lim_{t\to\infty} \mathcal{B}\Gamma\sin(\eta(t)) = \mathcal{B}\overline{P}_f, \tag{6}$$

where $\mathcal{B}\overline{P}_f$ is the desired net power flow. In case the power network does not contain cycles, Objective 2 is equivalent to $\lim_{t\to\infty} \Gamma\sin(\eta(t)) = \overline{P}_f$, such that the power flow on every line is identical to its desired value (see Remark 3 in Section 5). To be able to satisfy objectives 1 and 2, we make the following assumption on the feasibility of the control problem.

Assumption 2. (**Feasibility**) For a given constant $\overline{P}_d$, there exist a $\overline{u}$ and state $(\overline{f} = \mathbf{0}, \overline{\eta}, \overline{P}_t, \overline{P}_g)$ that satisfies

$$\begin{aligned} \mathbf{0} &= \mathcal{B}^T\mathbf{0} \\ \mathbf{0} &= -K_p^{-1}\mathbf{0} + \overline{P}_t - \overline{P}_d - \mathcal{B}\Gamma\sin(\overline{\eta}) \\ \mathbf{0} &= -\overline{P}_t + \overline{P}_g \\ \mathbf{0} &= -R^{-1}\mathbf{0} - \overline{P}_g + \overline{u}, \end{aligned} \tag{7}$$

where $\mathcal{B}\Gamma\sin(\overline{\eta}) = \mathcal{B}\overline{P}_f$.

We are now in a position to formulate the control problem:

Let Assumptions 1 and 2 hold. Given system (3)*, design a decentralized control scheme, providing a continuous control input, capable of guaranteeing that the controlled system is asymptotically stable with zero steady state frequency deviation, maintaining, at the steady state, the scheduled (net) power flows.*

4. THE PROPOSED SOLUTION

In this section the well established SSOSM controller proposed in Bartolini et al. (1998a) is applied, in a decentralized way, to the power network augmented with an additional state variable $\theta \in \mathbb{R}^n$ that enables a further tuning of the transient behaviour of the system. Its dynamics is

$$T_\theta \dot{\theta} = -\theta + P_t. \tag{8}$$

We select the sliding variables vector $\sigma \in \mathbb{R}^n$ as

$$\sigma = M_1 f + M_2 P_t + M_3 P_g + M_4 \theta + M_5 \mathcal{B}(\Gamma \sin(\eta) - \overline{P}_f), \tag{9}$$

where $M_1, \dots M_5$ are constant $n \times n$ diagonal matrices. The permitted values for $M_1, \dots M_5$ follow from the stability analysis in Section 5.

Remark 1. (**Local measurements**) Because $M_1, \dots, M_5$ are diagonal matrices, each sliding variable σ_i is defined by only local variables at node i.

We now continue by describing the controller that guarantees the convergence to the sliding manifold $\sigma = \dot{\sigma} = \mathbf{0}$. Since the system relative degree [2] is equal to 1, then, in order to obtain a continuous control input, the SSOSM control algorithm can be applied by artificially increasing the relative degree of the system. To do this, we define two auxiliary variables $\xi_1 = \sigma$ and $\xi_2 = \dot{\sigma}$, and build the so-called auxiliary system as follows

$$\begin{cases} \dot{\xi}_1 = \xi_2 \\ \dot{\xi}_2 = \phi + g w \\ \dot{u} = w, \end{cases} \tag{10}$$

where ξ_2 is not measurable, since, according to Assumption 1, P_d is unknown. Bearing in mind (9) and that $\ddot{\sigma} = \phi + g w$, it follows that $\phi \in \mathbb{R}^n$ and $g \in \mathbb{R}^{n \times n}$ are given by

$$\begin{aligned} \phi = &\Big(M_1 T_p^{-2} + M_3 R^{-1} T_p^{-1} T_g^{-1} - M_2 R^{-1} T_t^{-1} T_g^{-1} \\ &+ M_3 R^{-1} T_g^{-2}\Big) f - \Big(M_1 K_p T_p^{-2} + M_3 K_p R^{-1} T_p^{-1} T_g^{-1} \\ &+ M_1 K_p T_p^{-1} T_t^{-1} - M_2 T_t^{-2} + M_4 T_t^{-1} T_\theta^{-1} \\ &+ M_4 T_\theta^{-2}\Big) P_t + \Big(M_1 K_p T_p^{-1} T_t^{-1} - M_2 T_t^{-2} \\ &- M_2 T_t^{-1} T_g^{-1} + M_3 T_g^{-2} + M_4 T_t^{-1} T_\theta^{-1}\Big) P_g \\ &+ \Big(M_2 T_t^{-1} - M_3 T_g^{-1}\Big) T_g^{-1} u + \Big(M_1 T_p^{-1} \\ &+ M_3 R^{-1} T_g^{-1}\Big) \Big(K_p T_p^{-1} \overline{P_d} + K_p T_p^{-1} \mathcal{B} \Gamma \sin(\eta)\Big) \\ &- M_1 K_p T_p^{-1} \mathcal{B} \Gamma \tfrac{d}{dt} \sin(\eta) + M_5 \mathcal{B} \Gamma \tfrac{d^2}{dt} \sin(\eta) \\ &+ M_4 T_\theta^{-2} \theta, \\ g = \ & M_3 T_g^{-1}. \end{aligned} \tag{11}$$

[2] The relative degree is the minimum order r of the time derivative $\sigma_i^{(r)}, i \in \{1, \dots, n\}$, of the sliding variable associated to the i-th node in which the control $u_i, i \in \{1, \dots, n\}$, explicitly appears.

Note that, ϕ, g are uncertain due to the presence of the unmeasurable power demand P_d and possible parameter uncertainties. Referring to condition (4), and assuming that the parameter uncertainties are bounded, then ϕ and g can be bounded as

$$|\phi_i| \le \Phi_i, \ G_{\min_i} \le g_{ii} \le G_{\max_i}, \ i \in \mathcal{V} \tag{12}$$

Φ_i, $G_{\min_i}$ and $G_{\max_i}$, being positive constants. However, if the bounds Φ_i, $G_{\min_i}$ and $G_{\max_i}$ cannot be a-priori estimated, the adaptive version of the SSOSM algorithm proposed in Incremona et al. (2016) can be used to dominate the effect of the uncertainties.

To steer ξ_{1_i} and ξ_{2_i} to zero in a finite time even in presence of the uncertainties, the SSOSM algorithm (Bartolini et al. (1998a)) is used. Consequently, the control law for the i-th node is given by

$$w_i = -\alpha_i W_{\max_i} \operatorname{sgn}\left(\xi_{1_i} - \frac{1}{2}\xi_{1,\max_i}\right), \tag{13}$$

with

$$W_{\max_i} > \max\left(\frac{\Phi_i}{\alpha_i^* G_{\min_i}}; \frac{4\Phi_i}{3G_{\min_i} - \alpha_i^* G_{\max_i}}\right), \tag{14}$$

$$\alpha_i^* \in (0,1] \cap \left(0, \frac{3G_{\min_i}}{G_{\max_i}}\right). \tag{15}$$

In (13) the extremal values $\xi_{1,\max_i}$ can be detected by implementing for instance a peak detection as in Bartolini et al. (1998b). Moreover, note that the discontinuous SSOSM control law (13) only affects $\dot{\xi}_{2_i}$, and the control u_i fed into the governor of the node i is continuous.

5. STABILITY ANALYSIS AND MAIN RESULT

In this section we study the stability of the proposed control scheme. In order to prove stability we formulate two (nonrestrictive) assumptions.

Assumption 3. (**Desired sliding manifold**) Let $M_1 > 0$, $M_2 \ge 0$, $M_3 > 0$ diagonal matrices and let M_4 and M_5 be defined as

$$\begin{aligned} M_4 &= -(M_2 + M_3) \\ M_5 &= M_1 X, \end{aligned} \tag{16}$$

where X is a diagonal matrix satisfying [3]

$$\mathbf{0} < T_p K_p^{-1} - X T_p K_p^{-1} \mathcal{B} \Gamma [\cos(\overline{\eta})] \mathcal{B}^T K_p^{-1} T_p X, \tag{17}$$

and

$$\begin{aligned} \mathbf{0} < K_p^{-1} &- \frac{1}{4} K_p^{-1} X K_p^{-1} \\ &- \frac{1}{2}\big(T_p K_p^{-1} X \mathcal{B} \Gamma [\cos(\eta)] \mathcal{B}^T \\ &+ \mathcal{B} \Gamma [\cos(\eta)] \mathcal{B}^T X K_p^{-1} T_p\big). \end{aligned} \tag{18}$$

Remark 2. (**Required information on the network topology**) The value of X needs to be calculated once for the whole network and can be determined offline. The obtained value of X_{ii} needs then to be transmitted to control area i. Since all M_i are diagonal, the proposed control scheme is fully decentralized once the value of X is obtained. We note that (17) and (18) have the form of an algebraic Riccati inequality and a Lyapunov inequality respectively and efficient numerical methods exist to find a diagonal solution X. To facilitate a distributed controller

[3] Let $[\cos(\eta)]$ denote the $m \times m$ diagonal matrix $\operatorname{diag}\{\cos(\eta_1), \dots, \cos(\eta_m)\}$.

design that improves the scalability of the proposed solution, we provide a distributed method to determine a value of X satisfying (17) and (18) in Subsection 5.1.

The following assumption is made on the differences of voltage angles at steady state that is generally satisfied under normal operating conditions of the power network.

Assumption 4. (**Steady state voltage angles**) The differences in voltage angles in (7) satisfy

$$\overline{\eta} \in (-\frac{\pi}{2}, \frac{\pi}{2})^m. \tag{19}$$

The restrictions on M_i and $\overline{\eta}$ are required to apply LaSalle's invariance principle in Theorem 1.

Lemma 1. (**Convergence to the sliding manifold**) Let Assumption 1 hold. System (3) augmented with (8) converges in a finite time t_r to the sliding manifold where

$$\begin{aligned} P_g = &-M_3^{-1}(M_1 f + M_2 P_t + M_4\theta \\ &+ M_5\mathcal{B}(\Gamma\sin(\eta) - \overline{P}_f)). \end{aligned} \tag{20}$$

Proof. The proof is omitted due to space constraints.

Exploiting relation (20), the equivalent system on the sliding manifold is as follows:

$$\begin{aligned} \dot{\eta} &= \mathcal{B}^T f \\ T_p K_p^{-1}\dot{f} &= -K_p^{-1} f + P_t - \overline{P}_d - \mathcal{B}\Gamma\sin(\eta) \\ M_1^{-1}M_3T_t\dot{P}_t &= -M_1^{-1}(M_2+M_3)P_t - M_1^{-1}M_4\theta - f \\ &\quad - M_1^{-1}M_5\mathcal{B}(\Gamma\sin(\eta) - \overline{P}_f) \\ T_\theta\dot{\theta} &= -\theta + P_t \\ \sigma &= \mathbf{0}, \end{aligned} \tag{21}$$

where we include the auxiliary system (8).

As a consequence of Assumption 2 there exists a $(\overline{f} = \mathbf{0}, \overline{\eta}, \overline{P}_t, \overline{\theta})$ satisfying

$$\begin{aligned} \mathbf{0} &= \mathcal{B}^T\mathbf{0} \\ \mathbf{0} &= -K_p^{-1}\mathbf{0} + \overline{P}_t - \overline{P}_d - \mathcal{B}\Gamma\sin(\overline{\eta}) \\ \mathbf{0} &= -M_1^{-1}(M_2+M_3)\overline{P}_t - M_1^{-1}M_4\overline{\theta} - \mathbf{0} \\ &\quad - M_1^{-1}M_5\mathcal{B}(\Gamma\sin(\overline{\eta}) - \overline{P}_f) \\ \mathbf{0} &= -\overline{\theta} + \overline{P}_t \\ \sigma &= \mathbf{0}, \end{aligned} \tag{22}$$

where in (7), $\overline{P}_g = \overline{\theta} = \overline{u}$.

To show the desired convergence properties of the equivalent system (21) we consider the function

$$\begin{aligned} S(f,\eta,P_t,\theta) = &\frac{1}{2}f^T T_p K_p^{-1} f - \mathbb{1}_m^T\Gamma\cos(\eta) \\ &+ f^T T_p K_p^{-1} X\mathcal{B}\Gamma\sin(\eta) \\ &+ \frac{1}{2}P_t^T M_1^{-1}M_3T_tP_t \\ &+ \frac{1}{2}\theta^T M_1^{-1}(M_2+M_3)T_\theta\theta, \end{aligned} \tag{23}$$

that consists of an energy function of the power network (Trip et al. (2016)), a cross-term and common quadratic functions for the states of the turbine and the auxiliary dynamics. The stability of the system is then proven using an incremental storage function that is the Bregman distance (Bregman (1967)) associated to the function (23). The Bregman distance associated to S is defined as (notice the use of calligraphic $\mathcal{S}$):

$$\begin{aligned} \mathcal{S} = &S(f,\eta,P_t,\theta) - S(\mathbf{0},\overline{\eta},\overline{P}_t,\overline{\theta}) \\ &- \frac{\partial S}{\partial f}\Big|_{f=\mathbf{0}}^T (f-\mathbf{0}) - \frac{\partial S}{\partial \eta}\Big|_{\eta=\overline{\eta}}^T(\eta-\overline{\eta}) \\ &- \frac{\partial S}{\partial P_t}\Big|_{P_t=\overline{P}_t}^T (P_t-\overline{P}_t) - \frac{\partial S}{\partial \theta}\Big|_{\theta=\overline{\theta}}^T(\theta-\overline{\theta}) \\ = &\frac{1}{2}f^T T_p K_p^{-1} f \\ &- \mathbb{1}^T\Gamma\cos(\eta) + \mathbb{1}^T\Gamma\cos(\overline{\eta}) - (\Gamma\sin(\overline{\eta}))^T(\eta-\overline{\eta}) \\ &+ f^T T_p K_p^{-1} X\mathcal{B}(\Gamma\sin(\eta) - \Gamma\sin(\overline{\eta})) \\ &+ \frac{1}{2}(P_t-\overline{P}_t)^T M_1^{-1}M_3T_t(P_t-\overline{P}_t) \\ &+ \frac{1}{2}(\theta-\overline{\theta})^T M_1^{-1}(M_2+M_3)T_\theta(\theta-\overline{\theta}), \end{aligned} \tag{24}$$

where $(\mathbf{0}, \overline{\eta}, \overline{P}_t, \overline{\theta})$ satisfies (22). We remark that the Bregman distance $\mathcal{S}$ is equal to S minus the first order Taylor expansion of S around $(\mathbf{0}, \overline{\eta}, \overline{P}_t, \overline{\theta})$. We now derive two useful properties of $\mathcal{S}$, namely that $\mathcal{S}$ has a local minimum at $(\mathbf{0}, \overline{\eta}, \overline{P}_t, \overline{\theta})$ and that $\dot{\mathcal{S}} \leq 0$.

Lemma 2. (**Local minimum of $\mathcal{S}$**) Let Assumptions 2–5 hold. Then $\mathcal{S}$ has a local minimum at $(\mathbf{0}, \overline{\eta}, \overline{P}_t, \overline{\theta})$.

Proof. Since $\mathcal{S}$ is a Bregman distance associated to (23) it is sufficient to show that (23) is convex at the point $(\mathbf{0}, \overline{\eta}, \overline{P}_t, \overline{\theta})$ in order to infer that $\mathcal{S}$ has a local minimum at that point. We consider therefore the Hessian matrix $H(S(f,\eta,P_t,\theta))$, evaluated at $(\mathbf{0}, \overline{\eta}, \overline{P}_t, \overline{\theta})$, which we briefly denote $\overline{H}(S)$. A straightforward calculation shows that

$$\overline{H}(S) = \begin{bmatrix} Q & \mathbf{0} \\ \mathbf{0} & M \end{bmatrix}, \tag{25}$$

with

$$Q = \begin{bmatrix} T_pK_p^{-1} & T_pK_p^{-1}X\mathcal{B}\Gamma[\cos(\overline{\eta})] \\ [\cos(\overline{\eta})]\Gamma\mathcal{B}^T X K_p^{-1}T_p & \Gamma[\cos(\overline{\eta})] \end{bmatrix} \tag{26}$$

$$M = \begin{bmatrix} M_1^{-1}M_3T_t & \mathbf{0} \\ \mathbf{0} & M_1^{-1}(M_2+M_3)T_\theta \end{bmatrix}. \tag{27}$$

It is immediate to see that $M > \mathbf{0}$, such that $\overline{H}(S) > \mathbf{0}$ if and only if $Q > \mathbf{0}$. Since $\Gamma[\cos(\overline{\eta})] > \mathbf{0}$ as a result of Assumption 4, it is sufficient that the Schur complement of block $\Gamma[\cos(\eta)]\big|_{\eta=\overline{\eta}}$ of matrix Q satisfies

$$\mathbf{0} < T_pK_p^{-1} - XT_pK_p^{-1}\mathcal{B}\Gamma[\cos(\overline{\eta})]\mathcal{B}^T K_p^{-1}T_pX. \tag{28}$$

The claim then follows from Assumption 3. ■

Lemma 3. (**Evolution of $\mathcal{S}$**) Let Assumptions 2–5 hold. Then $\dot{\mathcal{S}} \leq 0$.

Proof. One can verify that

$$\begin{aligned} \dot{\mathcal{S}} = &-\begin{pmatrix} f \\ \mathcal{B}\Gamma(\sin(\eta) - \sin(\overline{\eta})) \end{pmatrix}^T Z \begin{pmatrix} f \\ \mathcal{B}\Gamma(\sin(\eta) - \sin(\overline{\eta})) \end{pmatrix} \\ &- (P_t-\theta)^T M_1^{-1}(M_2+M_3)(P_t-\theta), \end{aligned} \tag{29}$$

where we exploited (22) and define

$$Z = \begin{bmatrix} K_p^{-1} - T_p K_p^{-1} X \mathcal{B}\Gamma[\cos(\eta)]\mathcal{B}^T & \frac{1}{2}K_p^{-1}X \\ \frac{1}{2}XK_p^{-1} & X \end{bmatrix}. \quad (30)$$

Since $X > \mathbf{0}$, it follows that $\dot{\mathcal{S}} \leq 0$ if the Schur complement of block X of matrix $\frac{1}{2}(Z + Z^T)$ satisfies

$$\mathbf{0} < K_p^{-1} - \frac{1}{4}K_p^{-1}XK_p^{-1} - \frac{1}{2}(T_pK_p^{-1}X\mathcal{B}\Gamma[\cos(\eta)]\mathcal{B}^T + \mathcal{B}\Gamma[\cos(\eta)]\mathcal{B}^TXK_p^{-1}T_p). \quad (31)$$

The claim then follows from Assumption 3. ■

Now, we can prove the main result of this paper concerning the evolution of the augmented system controlled via the proposed SSOSM control strategy.

Theorem 1. (**Main result.**) Let Assumptions 1–5 hold. Consider system (3), augmented with the integrators (8) and controlled via (9)–(15). Then, the solutions of the closed-loop system starting in a neighbourhood of the equilibrium $(\overline{f} = \mathbf{0}, \overline{\eta}, \overline{P}_t, \overline{P}_g)$ approach the set where $\overline{f} = \mathbf{0}$ and $\mathcal{B}\Gamma\sin(\overline{\eta}) = \mathcal{B}\overline{P}_f$, where $\mathcal{B}\overline{P}_f$ is the desired net power exchanged by the control areas.

Proof. The proof follows from invoking an invariance principle and is omitted due to space constraints.

Remark 3. (**Acyclic network topologies.**) In case the topology of the power network does not contain any cycles, we have that the corresponding incidence matrix $\mathcal{B}$ has full column rank and therefore has a left-inverse satisfying $\mathcal{B}^+\mathcal{B} = I$, such that we can conclude from Theorem 1 that the system approaches the set where

$$\mathcal{B}\Gamma\sin(\overline{\eta}) = \mathcal{B}\overline{P}_f \implies \Gamma\sin(\overline{\eta}) = \overline{P}_f. \quad (32)$$

5.1 A distributed method to determine X.

In this subsection we provide a distributed method to determine a possible value of X that satisfies (17) and (18). For the sake of brevity the corresponding proofs are omitted.

Lemma 4. (**Satisfying (17).**) If $X = \epsilon_1 K_p T_p^{-1}$, with

$$\epsilon_1 < \min_{i\in\mathcal{V}} \left(\sqrt{\frac{T_{pi}}{2K_{pi}\sum_{k\in\mathcal{N}_i}\Gamma_k}} \right), \quad (33)$$

then (17) is satisfied.

Lemma 5. (**Satisfying (18).**) If $X = \epsilon_2 K_p T_p^{-1}$, with

$$\epsilon_2 < \min_{i\in\mathcal{V}} \left(\frac{T_{pi}}{\frac{1}{2} + 2K_{pi}T_{pi}\sum_{k\in\mathcal{N}_i}\Gamma_k} \right). \quad (34)$$

then (18) is satisfied.

From Lemma 4 and Lemma 5 the following corollary is immediate:

Corollary 1. (**Satisfying (17) and (18).**) Let

$$X = \epsilon K_p T_p^{-1}, \quad (35)$$

with $\epsilon = \min\{\epsilon_1, \epsilon_2\}$, then (17) and (18) are satisfied.

The result of this subsection can be used as follows. Every control area determines an upper bound for ϵ using (33) and (34), and broadcasts it to the rest of the network. Using the minimum of all estimated upper bounds of ϵ it is ensured that Assumption 3 holds.

Table 2. Network parameters and power demand

		Area 1	Area 2	Area 3	Area 4
T_{pi}	(s)	21.0	25.0	23.0	22.0
T_{ti}	(s)	0.30	0.33	0.35	0.28
T_{gi}	(s)	0.080	0.072	0.070	0.081
K_{pi}	(Hz p.u.$^{-1}$)	120.0	112.5	115.0	118.5
R_i	(Hz p.u.$^{-1}$)	2.5	2.7	2.6	2.8
$T_{\theta i}$	(s)	0.1	0.1	0.1	0.1
$P_{di}(0)$	(p.u.)	0.010	0.014	0.012	0.013
$\overline{P}_{d_i}$	(p.u.)	0.020	0.028	0.024	0.026

6. SIMULATION RESULTS

In this section, the proposed control solution is assessed in simulation by implementing a power network partitioned into four control areas. The topology of the power network is represented in Figure 1, where the arrow on each edge indicates the positive direction of the power flow. The relevant network parameters of each area are provided in Table 2, where a base power of 1000 MW is assumed. The line parameters are $\gamma_1 = 0.54$ p.u., $\gamma_2 = 0.50$ p.u. and $\gamma_3 = 0.52$ p.u., while the scheduled power flows are $\overline{P}_{f1} = 0.015$ p.u., $\overline{P}_{f2} = 0.0125$ p.u. and $\overline{P}_{f3} = 0.01$ p.u. The matrices in (9) are chosen as $M_1 = 10I_4$, $M_2 = I_4$, $M_3 = 0.1I_4$, $M_4 = -(M_2 + M_3)$ and $M_5 = 0.5I_4$, $I_4 \in \mathbb{R}^{4\times4}$ being the identity matrix, while the control amplitude $W_{\max_i}$ and the parameter α_i^*, $i = 1, \ldots, 4$, in (13) are selected equal to 100 and 1, respectively. In simulation, at the initial time instant $t_0 = 0$ s the system is at the steady state with power demand $P_{di}(0)$. Then, at the time instant $t = 2$ s, the power demand in each area becomes $\overline{P}_{di}$ (see Table 2). From Figure 2, one can observe that the frequency deviation converges asymptotically to zero after a transient during which the frequency drops because of the increasing load. Moreover, one can note that the controllers increase the power generation in order to reach

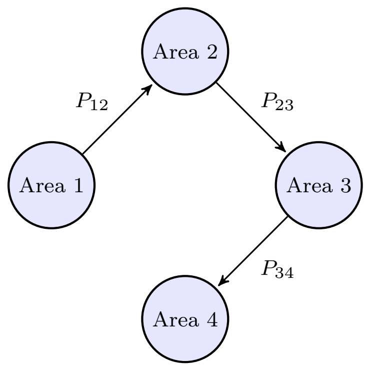

Fig. 1. Scheme of the considered power network partitioned into 4 control areas, where $P_{ij} = \frac{V_i^\star V_j^\star}{X_{ij}}\sin(\delta_i - \delta_j)$. The arrows indicate the positive direction of the power flows through the power network.

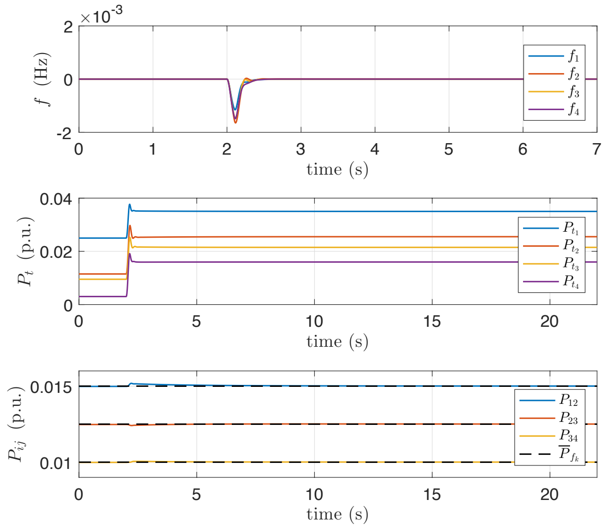

Fig. 2. Time evolution of the frequency deviation, power generation and power flows. The power demand changes at the time instant $t = 2\,\mathrm{s}$.

again a zero steady state frequency deviation, maintaining, at the steady state, the scheduled power flows $\overline{P}_{fk}$ on each line.

7. CONCLUSIONS

A decentralized Suboptimal Second Order Sliding Mode control scheme is proposed for Automatic Generation Control (AGC). We considered a power network partitioned into control areas, where each area is modelled by an equivalent generator including second order turbine-governor dynamics, and where the areas are nonlinearly coupled through the power flows. Relying on stability considerations made on the basis of an incremental energy (storage) function, a suitable sliding manifold is designed. Asymptotic convergence is proven to the state where the frequency deviation is zero and where the power flows are regulated towards their desired values.

REFERENCES

Apostolopoulou, D., Domínguez-García, A.D., and Sauer, P.W. (2016). An assessment of the impact of uncertainty on automatic generation control systems. *IEEE Transactions on Power Systems*, 31(4), 2657–2665.

Bartolini, G., Ferrara, A., and Usai, E. (1998a). Chattering avoidance by second-order sliding mode control. *IEEE Transactions on Automatic Control*, 43(2), 241–246.

Bartolini, G., Ferrara, A., and Usai, E. (1998b). On boundary layer dimension reduction in sliding mode control of SISO uncertain nonlinear systems. In *Proc. of the IEEE Internation Conference on Control Applications*, volume 1, 242 –247 vol.1. Trieste, Italy.

Bartolini, G., Ferrara, A., Levant, A., and Usai, E. (1999). *On second order sliding mode controllers*, 329–350. Springer London, London.

Bregman, L. (1967). The relaxation method of finding the common point of convex sets and its application to the solution of problems in convex programming. *USSR Computational Mathematics and Mathematical Physics*, 7(3), 200 – 217.

Chang, C. and Fu, W. (1997). Area load frequency control using fuzzy gain scheduling of pi controllers. *Electric Power Systems Research*, 42(2), 145 – 152.

Cucuzzella, M., Trip, S., De Persis, C., and Ferrara, A. (2017). Distributed second order sliding modes for optimal load frequency control. In *Proc. American Control Conf.* Seattle, WA, USA.

Dong, L. (2016). Decentralized load frequency control for an interconnected power system with nonlinearities. In *Proc. of the 2016 American Control Conference (ACC)*, 5915–5920.

Edwards, C. and Spurgen, S.K. (1998). *Sliding Mode Control: Theory and Applications*. Taylor and Francis, London, UK.

Ersdal, A.M., Imsland, L., and Uhlen, K. (2016). Model predictive load-frequency control. *IEEE Transactions on Power Systems*, 31(1), 777–785.

Ha, Q.P. (1998). A fuzzy sliding mode controller for power system load-frequency control. In *Knowledge-Based Intelligent Electronic Systems*, volume 1, 149–154 vol.1.

Incremona, G.P., Cucuzzella, M., and Ferrara, A. (2016). Adaptive suboptimal second-order sliding mode control for microgrids. *International Journal of Control*, 1–19.

Mi, Y., Fu, Y., Wang, C., and Wang, P. (2013). Decentralized sliding mode load frequency control for multi-area power systems. *IEEE Transactions on Power Systems*, 28(4), 4301–4309.

Mi, Y., Fu, Y., Li, D., Wang, C., Loh, P.C., and Wang, P. (2016). The sliding mode load frequency control for hybrid power system based on disturbance observer. *International Jorunal of Electrical Power and Energy Systems*, 74, 446 – 452.

Prasad, S., Purwar, S., and Kishor, N. (2015). On design of a non-linear sliding mode load frequency control of interconnected power system with communication time delay. In *Proc. of the IEEE Conference on Control Applications*, 1546–1551.

Trip, S., Bürger, M., and De Persis, C. (2016). An internal model approach to (optimal) frequency regulation in power grids with time-varying voltages. *Automatica*, 64, 240 – 253.

Utkin, V. and Lee, H. (2006). Chattering problem in sliding mode control systems. *IFAC Proceedings Volumes, 2nd IFAC Conference on Analysis and Design of Hybrid Systems*, 39(5), 1 –.

Utkin, V.I. (1992). *Sliding Modes in Control and Optimization*. Springer-Verlag.

Vrdoljak, K., Perić, N., and Petrović, I. (2010). Sliding mode based load-frequency control in power systems. *Electrocal Power Systems Research*, 80(5), 514 – 527.

Zribi, M., Al-Rashed, M., and Alrifai, M. (2005). Adaptive decentralized load frequency control of multi-area power systems. *International Jorunal on Electrical Power and Energy Systems*, 27(8), 575 – 583.